Supplementary Information (SI) for Journal of Materials Chemistry A.

Supporting information

High-Efficiency All-Polymer Ternary Blends Enable Exceptional Thermal Stability in Organic Photovoltaics

Bing-Huang Jiang,[1‡] Zih-Ruei Huang,[1‡] Chun-Jen Su,[2] Zhong-En Shi,[1] Choon Kit Chan,[3] Yu-Chih Hsu,[4] Yang-Yen Yu,[*1,5] Chih-Ping Chen,[*1,5]

[1] *Department of Materials Engineering and Organic Electronics Research Center, Ming Chi University of Technology, New Taipei City 24301, Taiwan*
[2] *National Synchrotron Radiation Research Center, Hsinchu 300094, Taiwan*
[3] *Mechanical Engineering Department, Faculty of Engineering and Quantity Surveying, INTI International University, 71800 Nilai, Negeri Sembilan, Malaysia*
[4] *Somapex Biotech. Co. Ltd. Kaohsiung, Taiwan*
[5] *Center for Sustainability and Energy Technologies, Chang Gung University, Taoyuan City 33302, Taiwan*

[‡] B.-H. Jiang and Z.-R. Huang contributed equally to this work.

*Corresponding authors. E-mail: cpchen@mail.mcut.edu.tw; yyyu@mail.mcut.edu.tw

Experimental Section

The organic photovoltaic (OPV) devices were fabricated with a inverted structure of indium tin oxide (ITO)/ZnO/active layer/MoO_3/Ag. Photolithography was used to pattern the ITO glass substrate [Sanyo, Japan (6.4 Ω sq^{-1})] to define the active area of the device. The substrates were subsequently cleaned by sequential immersion in deionized water, acetone, and isopropanol, followed by ultrasonic treatment using a ultrasonic cleaner [LISSOME LS-300H] and drying at 140 °C for 30 minutes. A sol–gel ZnO precursor was prepared by stirring zinc acetate (3.15 g), ethanolamine (0.9 mL), and 2-methoxyethanol (29.1 mL) for three days. After filtration through a 0.45-μm filter, the ZnO precursor was deposited onto the oxygen plasma-cleaned ITO glass using a spin-coater at 3000 rpm for 30 s. The deposited layer was then annealed in air at 170 ^{O}C for 20 min. In preparing the active layer, PBQx-TF and D18 were individually dissolved in chlorobenzene (10 mg/ml) and stirred at 120 °C for 1 hour under nitrogen, resulting in the formation of the donor precursor solution. To prepare the donor blend precursor, PBQx-TF and D18 were dissolved in chlorobenzene (10 mg/ml) at different weight ratios (9:1, 8:2, and 7:3) and stirred at 120 °C for 1 hour under nitrogen. PY-IT was dissolved in a chloroform solution (10 mg/ml) containing 2% (v/v) 1-chloronaphthalene (CN) and stirred at 25 °C overnight under nitrogen, yielding the acceptor precursor solution. The donor precursors and the ITO/ZnO-coated substrate were preheated to 100 °C on a hotplate. Donor and acceptor precursor solutions were sequentially deposited by spin-coating at 3000 rpm for 30 s each, resulting in a total active layer thickness of approximately 110 nm. For the final device fabrication, a 3 nm layer of MoO_3 and a 100 nm layer of Ag were sequentially deposited onto the active layer via thermal evaporation under a vacuum pressure of less than 10^{-6} torr. The effective area of the device was determined to be 0.1 cm^2, defined by the overlap between the ITO and Ag layers. The layer structure of ITO/MoO_3/Active layer/MoO_3/Ag was used for hole-only devices, and ITO/ZnO/Active layer/C_{60}/Ag was used for electron-only devices. C_{60}, as received from Xi'an Yuri Solar without further purification, was deposited by thermal evaporation to a thickness of 30 nm on top of the active layer.

Measurements

The current density-voltage (J-V) characteristics of the OPVs were measured using a Keithley 2400 source meter, controlled via a computer interface, in conjunction with an Enlitech AAA-grade solar simulator under standard AM 1.5G illumination. The simulator allowed for tunable light intensity, adjustable between 10 and 100 mW/cm^2. External quantum efficiency (EQE) spectra were acquired with a photo response measurement system [QE-R3011, Enlitech], calibrated using certified silicon (Si) and germanium (Ge) photodetectors to ensure the accurate provision of monochromatic light. UV-Vis absorption spectra and photoluminescence (PL) spectra were recorded using a spectrometer [JASCO V-770] and an photoluminescence spectrometer [Edinburgh FLS1000], respectively. The thickness of each layer was measured using a surface profiler [Kosaka Laboratory, E200] or an atomic force microscope [Bruker Dimension Edge] operated in tapping mode. Surface energy measurements were conducted by employing water and diiodomethane as probe liquids, with surface energy values determined using Wu's method. The surface morphology of the charge transport and active layers was characterized at ambient conditions via tapping-mode AFM. The GIWAXS spectra of the blend films were collected at the TLS 23A beamline of the National Synchrotron Radiation Research Center (Taiwan), using an X-ray beam with an energy of 10.0 keV and an incident angle of 0.15°. The sample-to-detector distance was set to 188.55 mm. Furthermore, the optoelectronic properties of the OPV devices, including Photo-CELIV and transient photocurrent (TPC), were characterized using a comprehensive all-in-one characterization platform [Paios, Fluxim AG]. An integrated system ELCT-3010 (Enli Technology Co., Ltd., Taiwan) was used to record the electroluminescence (EL) and EQE_{EL} spectra. The Fourier transform photocurrent spectroscopy–EQE (FTPS-EQE) spectra of devices were recorded using an integrated system, PECT600 (Enli Technology Co., Ltd., Taiwan).

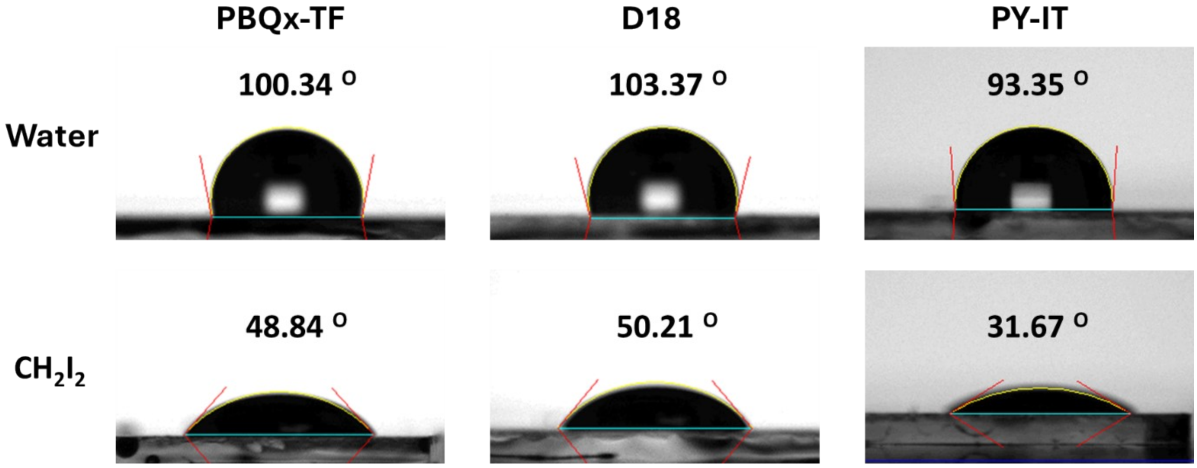

Figure S1. Contact angles of drops of water and diiodomethane for PBQx-TF, D18, and PY-IT.

Table S1. Surface energies, Flory–Huggins parameters (χ) and we between PBQx-TF, D18, and PY-IT.

Materials	Polar (mJ/m^2)	Dispersive (mJ/m^2)	Surface energy (mJ/m^2)	$\chi_{PBQx\text{-}TF:X}$	$\chi_{PY\text{-}IT:X}$	ω
PBQx-TF	1.44	36.20	37.64	-	0.146	-
D18	0.52	35.14	35.67	0.009	0.227	1.455
PY-IT	2.74	43.36	46.10	0.146	-	-

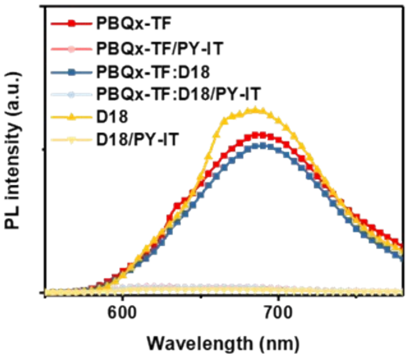

Figure S2. PL spectra of PBQx-TF, D18, PBQx-TF:D18, binary, and ternary blend films.

Table S2. Photovoltaic device parameters of OPVs prepared with various donor blend ratios.

PBQx-TF:D18	J_{SC} (mA cm^{-2})	V_{OC} (V)	FF (%)	PCE (%)
10:0	22.10	0.93	74.3	15.26
9:1	22.71	0.94	75.3	16.07
8:2	21.56	0.95	73.6	15.07
7:3	21.26	0.95	73.8	14.91
0:10	20.56	0.97	72.2	14.39

Table S3. Photovoltaic device parameters of ternary OPVs prepared with various thickness.

Thickness	J_{SC} (mA cm^{-2})	V_{OC} (V)	FF (%)	PCE (%)
130 nm	22.78	0.93	74.1	15.78
120 nm	22.71	0.94	75.3	16.07
110 nm	22.05	0.94	75.9	15.75

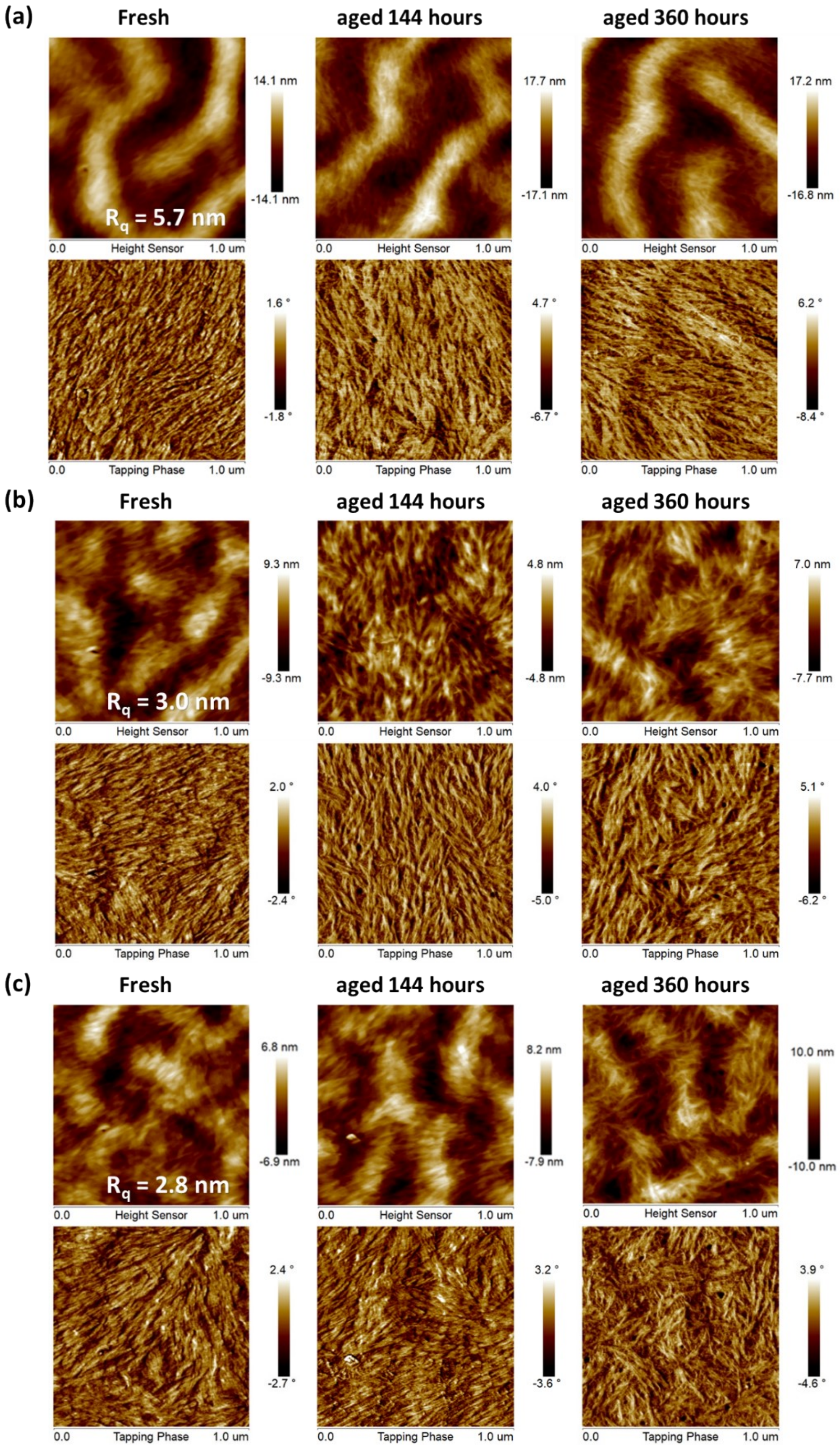

Figure S3. The AFM topographic and phase images of (a) PBQx-TF/PY-IT, (b) PBQx-TF:D18/PY-IT, and (c) D18/PY-IT blend films.

Table S4. Detailed Energy loss parameters of the binary and ternary OPVs.

Active layer	E_g [eV]	qV_{OC} [eV]	E_{loss} [eV]	E_{CT} [eV]	ΔE_{CT} [eV]	ΔE_{rad} [eV]	$\Delta E_{non\text{-}rad}$ [eV]	EQE_{EL}
PBQx-TF/PY-IT	1.480	0.92	0.560	1.425	0.055	0.277	0.228	1.40×10^{-4}
PBQx-TF:D18/PY-IT	1.477	0.95	0.527	1.447	0.030	0.274	0.223	1.71×10^{-4}
D18/PY-IT	1.480	0.97	0.510	1.435	0.045	0.278	0.187	6.83×10^{-4}

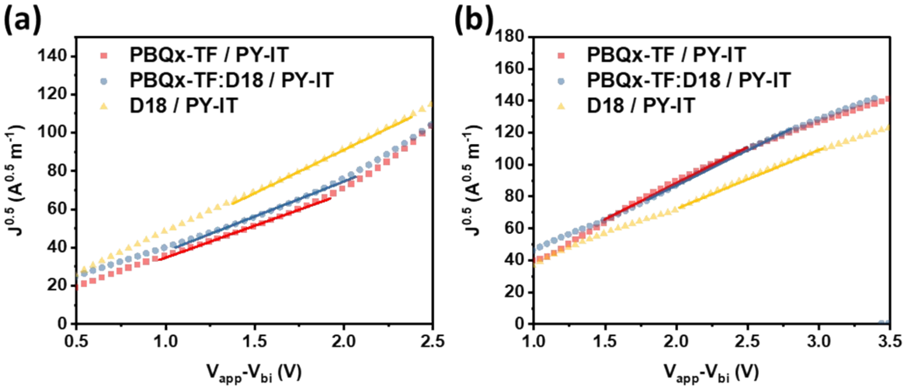

Figure S4. The $J^{0.5}$-V plots for the (a) hole-only and (b) electron-only devices.

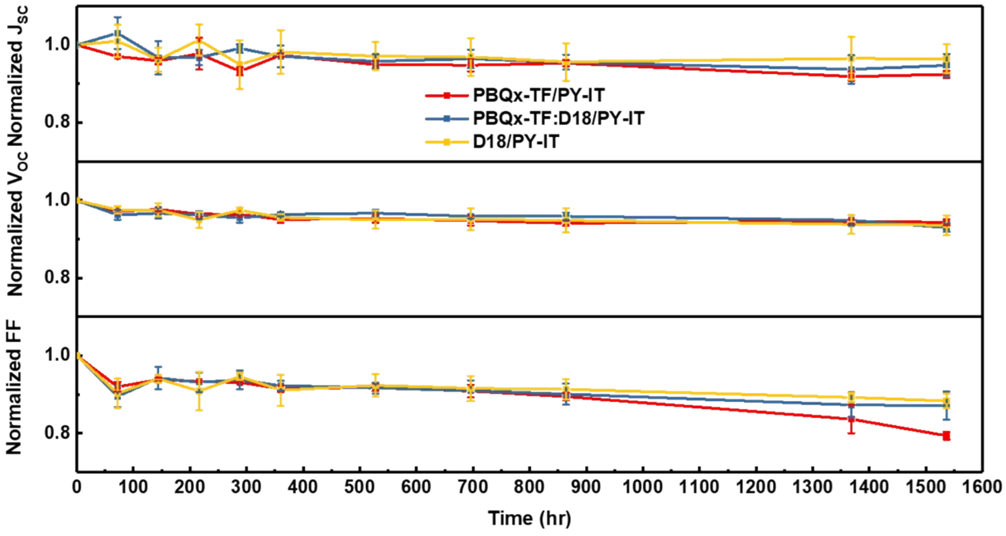

Figure S5. Normalized PV parameters of binary and ternary OPVs under thermal aging process at 120°C.

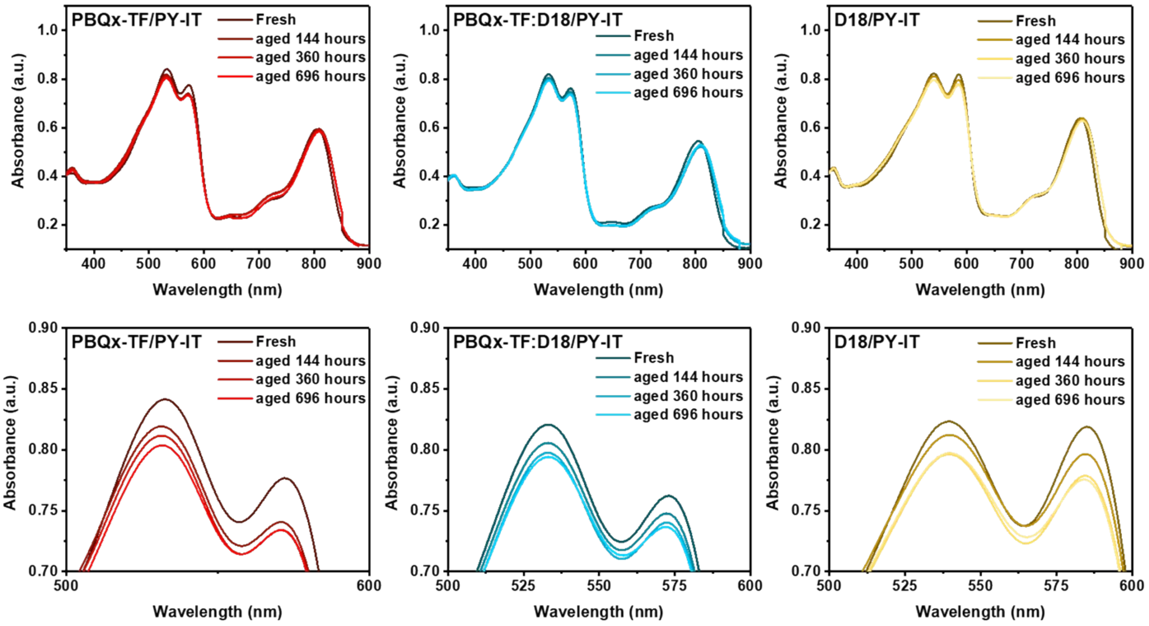

Figure S6. UV-vis absorption spectra of fresh/aged binary and ternary blend film.

Table S5. The thermal stability parameter of AP OPVs reported by previous literatures.

Active layer	The sample for thermal stability test	Aging conditions (°C)	Aged time (h)	Remain (%)	T_{80} (h)	Ref
PBDB-T : PJ1-H**c**	ITO/PEDOT:PSS/active layers	150	3	90	-	1
PBQx-TF:P2:PYIT	Unspecified	125	96	90	-	2
PBDB-T:PYTT-2	ITO/PEDOT:PSS/active layers	120	200	ca.98^{b}	-	3
PBDB-T:PYTT-1				90	-	
PTzBI-oF：PFA1	Unspecified	120	100	97.9	-	4
		100	8760	98	-	
PM6：PYBO-VH：PYBO-VF	Unspecified	120	-	-	1840^{a}	5
PBDB-T:P(BDT2BOY5-Cl)	Unspecified	100	100	90	-	6
PBDB-T:PYF-T:PZT	Unspecified	100	144	96.5	-	7
PBDB-T : PTClo-Y	Unspecified	90	160	87	-	8
PBDB-TF:B1:PY-IT	Unspecified	85	140	70	-	9
PM6:L15	Unspecified	85	2640	83.31	14000^{a}	10
QQ1: PY-IT	Unspecified	85	75	88	-	11
PBDB-T:PF5-Y5	Unspecified	85	41.7	75	-	12
PM6:PF1-TS4	ITO/ZnO/ active layer/MoO_3/Al	85	180	70	-	13
PBQx-TCl :	Unspecified	85	-	-	10600^{a}	14

PYFIT:P180k						
PM6:4Y-BO	Unspecified	85	-	-	2125[a]	15
PM6:PY-BO	Unspecified	85	512	80	512	
PBQx-TCl:PY-IT:PY-IV	Unspecified	85	-	-	ca.450[b]	16
PM6:PY-IT	Unspecified	80	200	71.3	-	17
PM6:PYF-T-o	Unspecified	80	250	90	-	18
PTzBI-Si:N2200	Unspecified	80	1000	93	-	19
PBDBT-BV 20 : N2200-TV 10	Unspecified	80	1.5	91	-	20

a Extrapolate to predict T_{80} time.

b Extracted from the thermal stability curve.

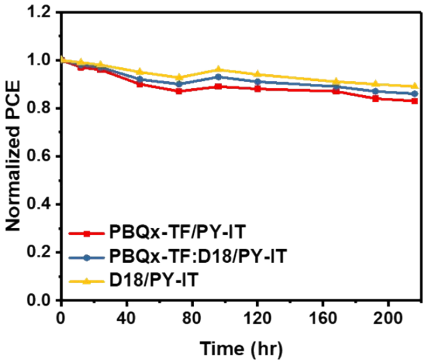

Figure S7. Normalized PCE of binary and ternary OPVs under continuous illumination in Ar-filled glovebox.

Reference

1. T. Jia, J. Zhang, W. Zhong, Y. Liang, K. Zhang, S. Dong, L. Ying, F. Liu, X. Wang and F. Huang, *Nano Energy*, 2020, **72**, 104718.
2. G. U. Kim, C. Choi, D. Jeong, D. J. Kim, T. N. L. Phan, S. Song, J. Park, T. S. Kim, Y. H. Kim and B. J. Kim, *Advanced Energy Materials*, 2023, **13**, 2302125.
3. T. Wang, R. Sun, W. Wang, H. Li, Y. Wu and J. Min, *Chemistry of Materials*, 2021, **33**, 761-773.
4. Z. Li, F. Peng, H. Quan, X. Qian, L. Ying and Y. Cao, *Chemical Engineering Journal*, 2022, **430**, 132711.
5. J.-W. Lee, J. Kim, T. H.-Q. Nguyen, D. C. Lee, Z. Tan, J. Park, T. N.-L. Phan, S. Cho and B. J. Kim, *Nano Energy*, 2024, **122**, 109338.
6. J. W. Lee, C. Sun, B. S. Ma, H. J. Kim, C. Wang, J. M. Ryu, C. Lim, T. S. Kim, Y. H. Kim and S. K. Kwon, *Advanced Energy Materials*, 2021, **11**, 2003367.

7. Z. Li, Y. Liang, L. Chen, J. Chen, F. Peng and L. Ying, *Chemical Engineering Journal*, 2023, **452**, 139228.
8. D. Chen, S. Liu, X. Hu, F. Wu, J. Liu, K. Zhou, L. Ye, L. Chen and Y. Chen, *Science China Chemistry*, 2022, **65**, 182-189.
9. F.-Z. Cui, Z. Chen, J.-W. Qiao, P. Lu, X. Du, W. Qin, H. Yin and X.-T. Hao, *ACS Energy Letters*, 2022, **7**, 3709-3717.
10. B. Liu, W. Xu, R. Ma, J. W. Lee, T. A. Dela Peña, W. Yang, B. Li, M. Li, J. Wu and Y. Wang, *Advanced Materials*, 2023, **35**, 2308334.
11. Z. Wang, X. Wang, L. Tu, H. Wang, M. Du, T. Dai, Q. Guo, Y. Shi and E. Zhou, *Angewandte Chemie*, 2024, **136**, e202319755.
12. Q. Fan, Q. An, Y. Lin, Y. Xia, Q. Li, M. Zhang, W. Su, W. Peng, C. Zhang and F. Liu, *Energy & Environmental Science*, 2020, **13**, 5017-5027.
13. Q. Fan, W. Su, S. Chen, T. Liu, W. Zhuang, R. Ma, X. Wen, Z. Yin, Z. Luo and X. Guo, *Angewandte Chemie International Edition*, 2020, **59**, 19835-19840.
14. K. Zhou, D. Han, K. Xian, S. Li, M. Gao, K. Zhang, B. Zhao, X. Li, Y. Chen and Y. Geng, *Energy & Environmental Science*, 2024, **17**, 5950-5961.
15. J. Wang, C. Sun, Y. Li, F. Bi, H. Jiang, C. Yang, X. Bao and J. Chu, *Nature Communications*, 2025, **16**, 1784.
16. R. Ma, H. Li, T. A. Dela Peña, X. Xie, P. W. K. Fong, Q. Wei, C. Yan, J. Wu, P. Cheng and M. Li, *Advanced Materials*, 2024, **36**, 2304632.
17. S. Yao, T. Yang, X. Shen, T. Li, B. Huang, H. Liu, X. Lu, T. Liu and B. Zou, *Journal of Materials Chemistry C*, 2022, **10**, 9723-9729.
18. H. Yu, M. Pan, R. Sun, I. Agunawela, J. Zhang, Y. Li, Z. Qi, H. Han, X. Zou and W. Zhou, *Angewandte Chemie International Edition*, 2021, **60**, 10137-10146.
19. K. Zhang, R. Xia, B. Fan, X. Liu, Z. Wang, S. Dong, H. L. Yip, L. Ying, F. Huang and Y. Cao, *Advanced Materials*, 2018, **30**, 1803166.
20. N. Y. Kwon, S. H. Park, H. Kang, Y. U. Kim, H. D. Chau, A. K. Harit, H. Y. Woo, H. J. Yoon, M. J. Cho and D. H. Choi, *ACS Applied Materials & Interfaces*, 2021, **13**, 16754-16765.